

## Comparison of wind power estimates from the ECMWF reanalyses with direct turbine measurements

Péter Kiss,<sup>1</sup> László Varga,<sup>2</sup> and Imre M. Jánosi<sup>1,a)</sup>

<sup>1</sup>*Department of Physics of Complex Systems, Loránd Eötvös University,*

*Pázmány P. s. 1/A, H-1117 Budapest, Hungary*

<sup>2</sup>*E.ON Hungária Ltd., Roosevelt tér 7-8, H-1051 Budapest, Hungary*

(Received 6 March 2009; accepted 22 May 2009; published online 11 June 2009)

Reanalysis data are rarely used for wind power estimates because of the limited spatial and temporal resolution. Here we report on a detailed comparison of wind speed and electric power time series recorded at a continental location in Hungary and estimates provided by the European Centre for Medium-Range Weather Forecasts (ECMWF) ERA-40 and Interim databases at nearby grid points. The results show that the temporal behavior is adequately represented in reanalysis records with damped magnitudes, as expected. However, characteristic shape differences in the wind speed histograms for turbine measurements and reanalysis hinder a perfect match of statistics. A satisfying agreement of histograms for measured and modeled output powers is achieved by scaling up surface wind speeds to have the same long time average value as for the turbine records. The presented calibration permits us to provide wind power estimates for large geographic areas, where the wind field is similarly coherent as around the test site. © 2009 American Institute of Physics. [DOI: [10.1063/1.3153903](https://doi.org/10.1063/1.3153903)]

### I. INTRODUCTION

The twitching of oil prices throughout the year 2008 or the latest Eastern European gas crisis in January 2009 has again boosted discussion on the future role of renewable energy sources. Over the past decade, the governments of leading industrial countries have appreciably supported the development of both solar and wind energies. In spite of this fact, renewable energy represents only 5%–6% of the total energy consumption among Organization for Economic Cooperation and Development countries.<sup>1</sup> Besides economic and technical questions, there is a primary interest in estimating the physical potential and limitations of various resources.

A recent comprehensive study on global wind energy potential by Archer and Jacobson is based on wind speed measurements at 7753 surface and 446 sounding stations.<sup>2</sup> They concluded that  $\sim 72$  TW ( $72 \times 10^{12}$  W) electricity<sup>3</sup> could be effectively generated using  $\sim 13\%$  of the locations around the world that have mean wind speeds of at least 6.9 m/s.<sup>2</sup> However, the spatial coverage of reporting stations was quite uneven; therefore large areas were under-represented in the estimates. An optimal global evaluation would require a dense measuring tower network and a waiting time of 5–10 years, but of course, this is not possible in practice. Landberg *et al.* listed eight alternative methods for wind resource estimate, starting from “folklore” to combined meso-/microscale modeling.<sup>4</sup> Global databases of winds (method 4 in Ref. 4) have become available within the past decade as a result of huge reanalysis efforts by various institutions such as the National Centers for Environmental Prediction/National Center for Atmospheric Research<sup>5,6</sup> or the European Centre for Medium-Range Weather Forecasts (ECMWF).<sup>7</sup> Measured surface wind data (at standard 10 m) over the ocean by buoys and satellites are assimilated in the reanalyses;<sup>7</sup> however, validation projects have revealed some statistical deficiencies in the extrapolated fields over the Arctic Ocean,<sup>8</sup> over the equatorial Indian Ocean,<sup>9</sup> or over a complex terrain.<sup>10</sup>

<sup>a)</sup> Author to whom correspondence should be addressed. Electronic mail: [janosi@lecco.elte.hu](mailto:janosi@lecco.elte.hu).

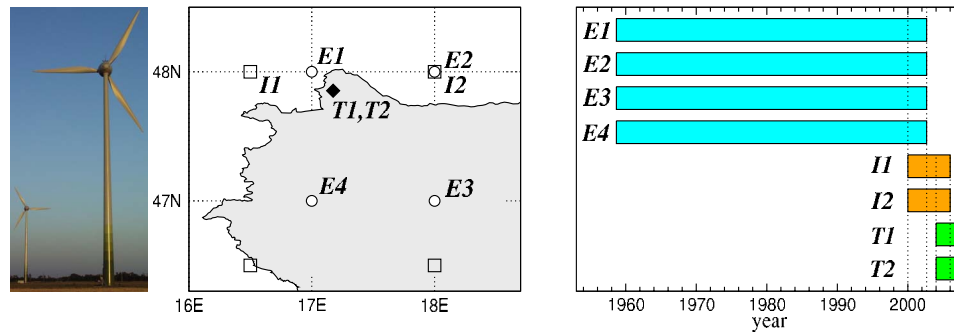


FIG. 1. Sketch of the geographic setting of the study area and timeline of the records. Heavy diamond indicates the location of the two Enercon E-40 wind turbines T1 and T2 ( $47.816^{\circ}$  N,  $17.174^{\circ}$  E), gray shading signs indicate Hungary, E1–E4 label the nearby ERA-40 grid points (empty circles), and I1 and I2 (empty squares) locate the grid points from the ERA-Interim database used for comparison. The timeline illustrates the overlapping periods 01/01/2000–08/31/2002 for E and I records and 01/01/2004–12/31/2005 for I and T time series. (Photograph: Sándor Zátanyi, <http://www.panoramio.com>)

In the absence of turbine-level (60–120 m) observations or model data, it is common practice to extrapolate surface wind data upward<sup>2,11–14</sup> or free-atmosphere fields downward.<sup>4,15,16</sup> In a recent study on wind power availability over Europe, Kiss and János<sup>17</sup> introduced a new empirical method using ECMWF ERA-40 wind velocity and geopotential records at the surface and at the 1000 hPa pressure levels. Their main conclusions on the strong spatial correlations and frequent global low-wind situations are not affected by the wind estimate at potential hub heights; however, numerical values of the aggregated average output are obviously sensitive to the method of extrapolation.

In this work, ECMWF reanalysis data are compared with direct measurements of wind speed and output power recorded at two wind turbines in the middle of the European continent. The results indicate a reasonably good agreement between measured and extrapolated wind speeds considering the temporal evolution; however, characteristic differences are present in the shape of wind speed histograms. Since the power curve of wind turbines can be considered as a highly nonlinear filter at estimating output from wind speeds, relatively small changes in the histogram can result in large deviations for the statistics of output power. Still, a simple matching of average values for wind speeds by a constant multiplier provides a surprisingly good estimate for the histogram of measured power.

## II. DATA SOURCES

In an earlier study,<sup>17</sup> ECMWF ERA-40 reanalysis data<sup>7</sup> for the  $u$  (eastward) and  $v$  (northward) orthogonal components of the horizontal wind field at 10 m above ground are evaluated for a time period of 44 years between 09/01/1958 and 08/31/2002. Four values are available each day for synoptic hours 00, 06, 12, and 18 universal time coordinated (UTC) at each geographic location. The spatial resolution is  $1^{\circ} \times 1^{\circ}$  (latitude/longitude), and the representation of subscale events is not attempted. Several statistical characteristics for the wind speed  $s = \sqrt{u^2 + v^2}$  are extracted for a subgrid covering the geographic area of Europe.<sup>18</sup> The present analysis is restricted to a single cell surrounding the site of reporting wind turbines, see Fig. 1.

High frequency wind speed (nacelle anemometer reading at 65 m above ground) and output power data at the geographic location  $47.816^{\circ}$  N,  $17.174^{\circ}$  E (near Mosonszolnok, Hungary) are available to us for a comparison (Fig. 1). 10 min average values are recorded for two neighboring Enercon E-40 wind turbines in the period 01/01/2004–12/31/2006. The proximity of the locations (the distance is 370 m) yielded very similar time series; significant differences originated from measuring errors, or hardware breakdowns indicated most often by zero power reading during high-wind periods, or finite electric output at zero recorded wind speeds.

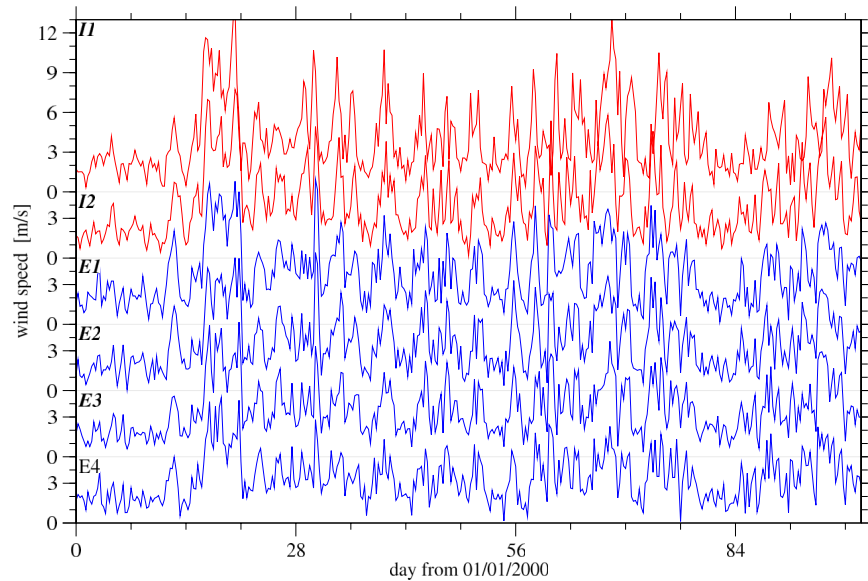


FIG. 2. Wind speed records for the  $I1$ ,  $I2$ , and  $E1$ – $E4$  grid points (see Fig. 1) in the first 100 days of the overlapping period.

Since there is no temporal overlap between the ERA-40 and turbine time series (Fig. 1), a direct comparison is not possible. Fortunately, the third generation reanalysis ECMWF ERA-Interim<sup>19</sup> has become available until the end of 2005 (at the time of finishing this work). There are some differences in data assimilation and use of observations between ERA-40 and ERA-Interim;<sup>19</sup> furthermore the spatial resolution decreased to  $1.5^\circ \times 1.5^\circ$  (latitude/longitude); however, the 6 h sampling remained the same as in ERA-40. Two grid points are close enough to the location of turbines (see Fig. 1); thus, time series in the period during 01/01/2000–12/31/2005 are used to bridge the temporal gap between ERA-40 and the turbine measurements (Fig. 1).

### III. COMPARISON OF WIND SPEED RECORDS

Figure 2 shows wind speed time series for the initial 100 days of the overlapping period at the sites  $I1$ ,  $I2$ , and  $E1$ ,  $\dots$ ,  $E4$  (note that  $I2$  and  $E2$  refer to the Interim and ERA-40 records for the same geographic grid point, see Fig. 1). It is easy to see that the wind speed changes quite homogeneously over the given area; the gross dynamical features are almost identical. The apparent synchrony can arise, on one hand, from the smooth orography: the area belongs to the Little Hungarian Plain, a low lying tectonic basin of approximately 8000 km<sup>2</sup> in northwestern Hungary, southwestern Slovakia, and eastern Austria. On the other hand, the 6 h time resolution of the records can easily hide shorter temporal shifts between the wind speed signals.

The same is true for the wind speed records at sites  $I1$ ,  $I2$ , and  $T1$ ,  $T2$  in the overlapping period of 2 years, see Fig. 3 (since  $T1$  and  $T2$  speeds are practically identical in the absence of technical failures, only the former is shown). Note that 6 h average values are determined from the turbine data series, where the time stamps are centered to the UTC sampling time of ERA-40 and Interim records. This is because the reanalysis wind fields are quite smooth (subgrid scale turbulence is not resolved); wind gusts and lulls are not represented. In Fig. 3, the agreement between the turbine measurements ( $h=65$  m) and surface wind speeds ( $h=10$  m) is not as strong as in Fig. 2; nevertheless the temporal evolution of the turbine record is properly reflected by the reanalysis.

In order to quantitatively characterize the strength of synchrony, we computed the usual two-point correlation matrix for the overlapping periods by

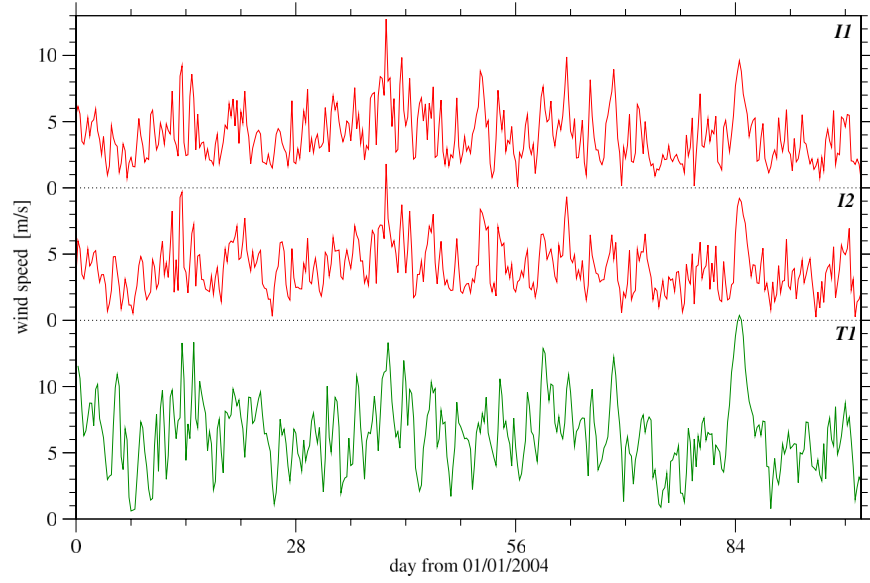


FIG. 3. The same as Fig. 2 for the  $I1$  and  $I2$  (red) and  $T1$  (green) records.

$$\text{Corr}(s_i, s_j) = \frac{\langle (s_i(t) - \bar{s}_i)(s_j(t) - \bar{s}_j) \rangle_t}{\sigma_i \sigma_j}, \quad (1)$$

where  $i, j \in \{E1, E2, E3, E4, I1, I2, T1, T2\}$ ,  $s(t)$  denotes the wind speed of average value  $\bar{s}$  and standard deviation  $\sigma$ , and  $\langle \cdot \rangle_t$  indicates temporal averaging. The results are shown in Table I. (The lower diagonal represents the geographic distances between the sites in units of kilometers.) It is worth to mention that the corresponding cross correlation functions (not shown here) exhibit a quick drop for nonzero time lags both in the negative and positive directions, which means that the wind field is essentially coherent in time windows of 6 h over the given area. The correlation matrix (Table I) seems to be consistent in the sense that larger spatial separation usually entails a lower correlation coefficient. The differences between ERA-40 and Interim records are characterized by the matrix element  $\text{Corr}(s_{E2}, s_{I2}) = 0.847$  for the same grid point.

We tested the effect of spatial interpolation with the records  $I1$  and  $I2$  by means of inverse squared distance weights<sup>20</sup> for the turbine location. Since the improvement was negligible, we used the original time series for further analysis.

Statistical differences are also present when the histograms of wind speeds are compared. Figure 4 illustrates the normalized empirical probability densities of wind speeds for each record.

TABLE I. Equal time two-point correlation [see Eq. (1)] matrix for the time series in the overlapping periods (upper diagonal) and geographic distance in units of km (lower diagonal, in parentheses).

	$E1$	$E2$	$E3$	$E4$	$I1$	$I2$	$T1$	$T2$
$E1$	1	0.929	0.824	0.873	0.797	0.772	...	...
$E2$	(74.6)	1	0.902	0.841	0.765	0.847	...	...
$E3$	(134.3)	(111.2)	1	0.913	0.716	0.820	...	...
$E4$	(111.2)	(134.3)	(76.1)	1	0.742	0.757	...	...
$I1$	(37.3)	(111.9)	(158.5)	(117.4)	1	0.880	0.768	0.743
$I2$	(74.6)	(0)	(111.2)	(134.3)	(111.9)	1	0.753	0.734
$T1$	...	...	...	...	(53.7)	(63.3)	1	0.971
$T2$	...	...	...	...	(53.7)	(63.3)	(0.4)	1

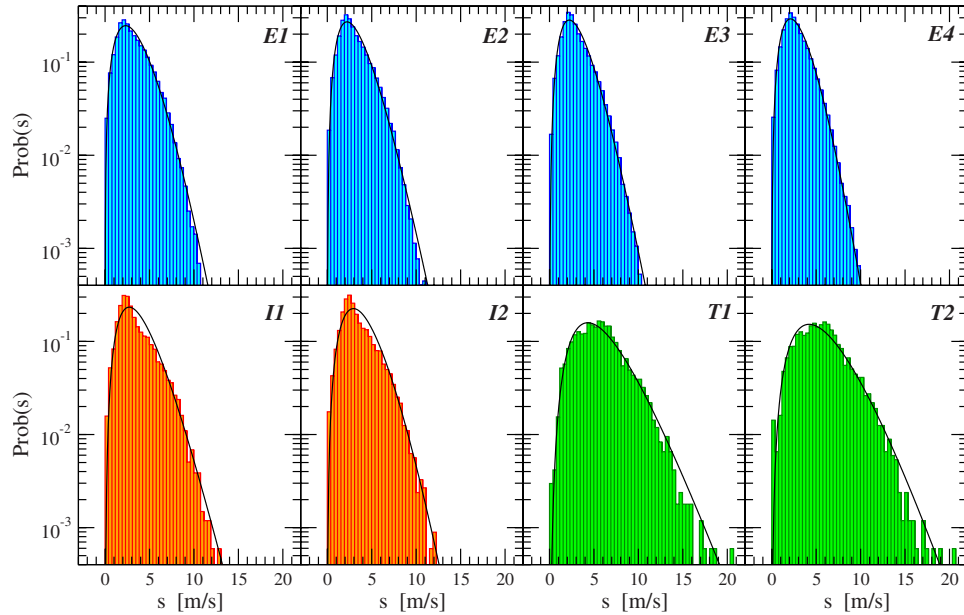


FIG. 4. Normalized histogram of wind speed  $s$  for the time series  $E1, E2, \dots, T2$  and fitted generalized gamma [see Eq. (2)] probability density functions (thin black lines). The empirical parameters are summarized in Table II.

Kiss and Jánosi obtained in a previous analysis<sup>18</sup> that the best functional fit for similar histograms over Europe is provided by the generalized gamma distribution, which has a probability density

$$P_{GG}(s; \beta, q, k) = \frac{k\beta^{(q+1)/k}}{\Gamma[(q+1)/k]} s^q \exp(-\beta s^k) \quad (2)$$

of three parameters  $\beta$ ,  $q$ , and  $k$  and a normalizing factor with the gamma function.<sup>21</sup> The effects of the two shape parameters  $q$  and  $k$  cannot be fully separated; nevertheless the asymptotic behavior on the left side (vanishing speed values) is a power law, while it is a stretched exponential on the right (large wind speeds). The empirical histograms are fitted by the standard method of maximum likelihood estimates;<sup>22,23</sup> the values of parameters are listed in Table II for each record. The fitted curves in Fig. 4 have very similar shapes; nevertheless the parameters can be quite different. This

TABLE II. Fitted parameters of the normalized wind speed probability distributions for the time series  $E1, E2, \dots, T2$ , see Fig. 4. The mean value  $\bar{s}$  and standard deviation  $\sigma$  are taken over the entire available record lengths (see Fig. 1), the parameters of the generalized gamma distribution [see Eq. (2)] are denoted by  $\beta$ ,  $q$ , and  $k$ , and the mode (most probable value) is  $m = (q/k\beta)^{1/k}$ . The second column ( $R_{T1}$ ) is the ratio of average wind speed  $\bar{s}_{T1}$  at the turbine  $T1$  and at the given site  $\bar{s}$ .

	$\bar{s}$ (m/s)	$R_{T1}$	$\sigma$ (m/s)	$\beta$	$q$	$k$	$m$ (m/s)
$E1$	3.19	1.79	1.75	0.306	1.404	1.411	2.306
$E2$	3.06	1.87	1.64	0.669	1.990	1.172	2.216
$E3$	2.99	1.91	1.56	0.704	2.145	1.184	2.219
$E4$	2.82	2.02	1.48	0.468	1.734	1.352	2.106
$I1$	3.43	1.66	1.96	0.758	2.423	1.084	2.712
$I2$	3.51	1.63	1.90	0.312	1.952	1.391	2.947
$T1$	5.71	1	2.67	0.790	3.195	0.975	4.302
$T2$	5.70	1.00	2.72	0.347	2.241	1.182	4.207

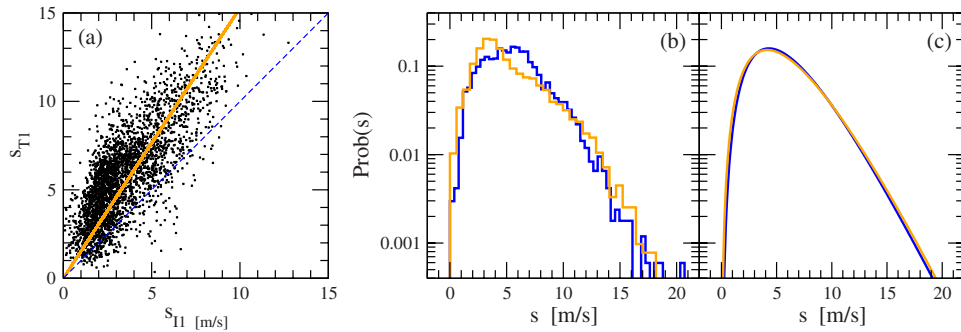


FIG. 5. (a) Scatter plot for the equal time wind speeds measured at sites  $I1$  and  $T1$ . The regression line has the slope of 1.529. (b) Normalized empirical wind speed histograms for the  $T1$  turbine measurements (dark, blue) and the transformed  $I1$  record (light, orange):  $s'_{I1} \rightarrow 1.529 \times s_{I1}$ . (c) The same as (b) for the fitted probability distributions.

is because  $\beta$ ,  $q$ , and  $k$  are very sensitive to small, sometimes hardly visible changes at the tails of the histograms.

The main difference between reanalysis and turbine histograms is that the latter exhibits significantly higher average value and width due to the increased elevation. It is well known that the shape of vertical wind profiles depends on many factors and changes with the weather; however, the basic behavior of the flow in the atmospheric boundary layer over a flat terrain of uniform roughness is known.<sup>24,25</sup> Nevertheless it is not easy to give an accurate quantitative estimate for wind speeds at higher levels, e.g., Archer and Jacobson<sup>2</sup> checked six different formulations for each location to obtain an acceptable fit. The overlapping time interval between the ERA-Interim reanalysis and turbine records allows to test the empirical relation between wind speed values at the surface (10 m) and at the hub height of 65 m. The equal time scatter plot for  $I1$  and  $T1$  time series is shown in Fig. 5(a); the linear relationship as a first approximation is suggested by the data. The effect of the simple linear transformation  $s'_{I1} \rightarrow 1.529 \times s_{I1}$  is illustrated in Figs. 5(b) and 5(c). While the fitted generalized gamma distributions collapse almost perfectly [Fig. 5(c)], the empirical histograms [Fig. 5(b)] exhibit characteristic differences already apparent in Fig. 4. The most probable empirical value (the peak) is shifted to larger speeds for turbine data with respect to an “ideal” generalized gamma curve; contrarily, the peak is shifted toward lower values for the reanalysis histogram. Actually, all of the empirical histograms in Fig. 4 seem to be a mixture of at least two unimodal distributions when a fit of really good quality is attempted. Such an attribute can be a consequence of the strong seasonality common in midlatitudes, where the different seasons are connected with different prevailing winds.<sup>26</sup>

#### IV. WIND ENERGY EXPLOITATION: MEASURED DATA

Figure 6 illustrates the smoothed output power measured directly at the turbines  $T1$  and  $T2$  in three working years. The two curves are pretty similar; significant differences are due to technical problems. It is remarkable that the apparent seasonality is very weak, and the fluctuations are huge in spite of the smoothing by a wide window of 1 week. The average load factor or capacity factor (the ratio of mean and rated output powers) around 21%–22% is considerably lower than at optimal off-shore sites,<sup>27–29</sup> in contempt of the geographic location of turbines belonging to the windiest region of Hungary.<sup>30–34</sup>

The standard method for estimating wind power from wind speed data is based on the empirical power curve<sup>35,36</sup> provided by the producers (see the power curves, e.g., <http://www.enercon.de>, <http://www.nordex-online.com>, <http://www.vestas.com>). The rated power of commercial turbines spans a wide range from a few kW to 6 MW; however, typical power curves share several other aspects. The cut-in wind speed  $s_{ci}$  is usually 2–5 m/s; then the curve exhibits a power-law range with an exponent value between 2 and 3. There is a crossover at around  $s_x \approx 11$ –15 m/s to a plateau (representing the rated power regime of active blade pitch control), and the cut-out wind speed  $s_{co}$  is 25 m/s for most constructions.

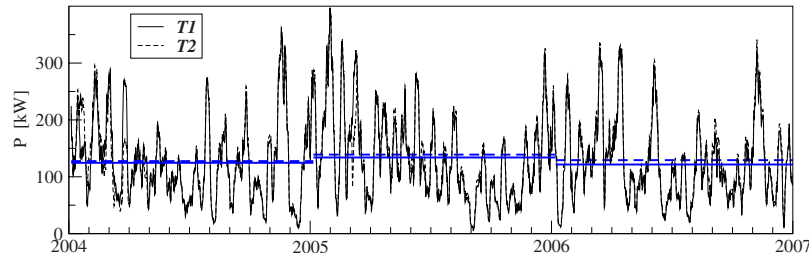


FIG. 6. Electric power output measured at the turbines  $T1$  (thin black line) and  $T2$  (dashed black line) in three consecutive years; high frequency (10 min) data are smoothed by 1008 point (1 week) running average. Horizontal (blue) lines indicate the annual averages. (Percentage values with respect to the rated power are  $20.76\% \pm 11.55\%$ ,  $22.33\% \pm 12.58\%$ , and  $20.27\% \pm 11.24\%$  for  $T1$  and  $21.26\% \pm 11.66\%$ ,  $23.16\% \pm 12.24\%$ , and  $21.55\% \pm 11.58\%$  for  $T2$ , respectively.)

The high frequency wind speed (Fig. 3) and output power (Fig. 6) time series permits constructing rather accurate power curves for the turbines  $T1$  and  $T2$ . Note that the only purpose of an operational form is to provide a smooth relationship between input (dimensionless speed) and output (dimensionless power) based entirely on measured data; therefore neither the mathematical forms nor the number of parameters are unique. The following functional form (shown in Fig. 7) provides a reasonable fit of recorded data:

$$P(s) = a_0(s - s_{ci})^\beta \quad \text{if } s_{ci} \leq s \leq s_x,$$

$$P(s) = \frac{a_1}{1 + \exp[-(s - b)^c]} \quad \text{if } s_x < s \leq s_{co}, \quad (3)$$

$$P(s) = 0 \quad \text{if } s < s_{ci} \quad \text{or} \quad s > s_{co}.$$

The constant values for turbine  $T1$  are  $s_{ci}=2.5$ ,  $s_x=10.0$ ,  $s_{co}=25.0$ ,  $\beta=2.14$ ,  $a_0=5.983$ ,  $a_1=622.0$ ,  $b=9.16$ , and  $c=1.05$  (since the variables  $s$  and  $P$  are normalized by their dimensions ( $1 \text{ ms}^{-1}$ ) and ( $1 \text{ kW}$ ), all the parameters are dimensionless quantities). Numerical values for

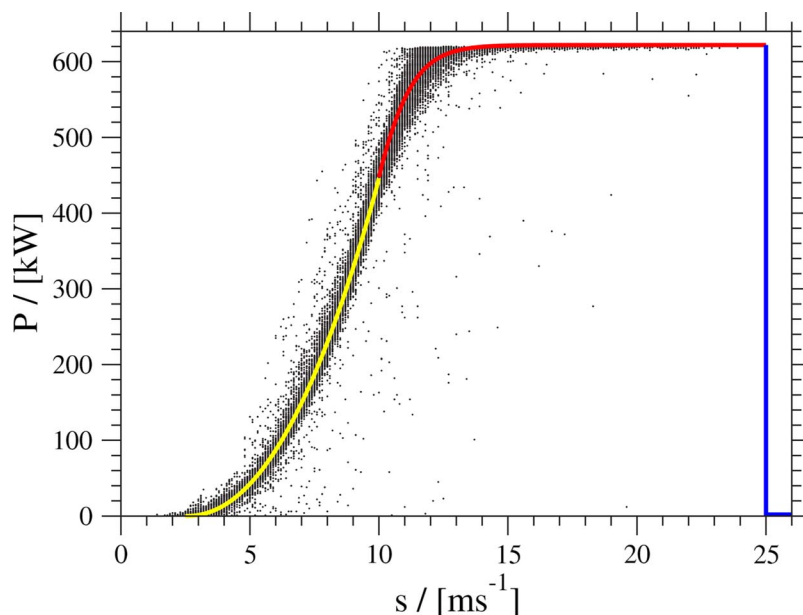


FIG. 7. Power curve fit Eq. (3) of high frequency (10 min) measured nacelle anemometer ( $h=65 \text{ m}$ ) data for  $T1$ .

turbine  $T2$  are very close to these. Note that  $a_1$  is slightly higher than the rated power for both fits, but this is common for most commercial generators, see the product data sheets.

## V. WIND ENERGY EXPLOITATION: ESTIMATES FROM WIND SPEED

Based on the fitted curve in Eq. (3), an estimate for output power can be given at the sites where wind speed records are available. A comparison between turbine measurements and modeled time series at seemingly distant geographic locations seems to be reasonable because of the strong spatial correlations revealed in Sec. III.

Estimated power data are produced in two steps. First, wind speed values referring to 10 m above ground are scaled up to the hypothetical hub height of 65 m by  $s' \rightarrow \alpha s$  using a constant factor  $\alpha$  (see Fig. 5). Second, model output representing 6 h average values is computed by Eq. (3) from the rescaled wind speed  $s'$ . A point-by-point comparison with turbine data is possible only for sites  $I1$  and  $I2$  in the overlapping period of 2 years (see Fig. 1). Time series for the first 100 days are shown in Fig. 8. The general behavior is similar to the wind speed curves in Fig. 3. The gross features are reproduced with apparent deviations in fine details.

Collating of statistical properties has shown that model time series produce systematically lower mean (annual) capacity factors than the measured values in Fig. 6. The reason is the marked difference in the histograms of the turbine and scaled reanalysis data shown in Fig. 5(b). The probability of wind speed in the range of [3–10] m/s is skewed to larger values for the turbines, while an opposite skew is apparent in the reanalysis data. Note that the very wind speed interval is critical, because small differences in numerical values are strongly exaggerated by the cubic behavior of the power curve (Fig. 7).

As we mentioned in Sec. III, the shape of wind speed histograms in Figs. 4 and 5(b) cannot be perfectly fitted by simple functional forms, because they seem to be mixed. For the same reason, an uncomplicated transformation resulting in an adequate collapse of the histograms in Fig. 5(b) is not possible. Nevertheless Fig. 5(a) suggests a relatively simple relationship between the heights of 10 and 65 m; therefore a systematic search of a proper multiplier is performed to obtain the best agreement between model and empirical capacity factors.

We have tested the mean, mode, and median of the wind speed histograms as possible scaling factors. Simple statistical comparison of measured and modeled power outputs revealed that the

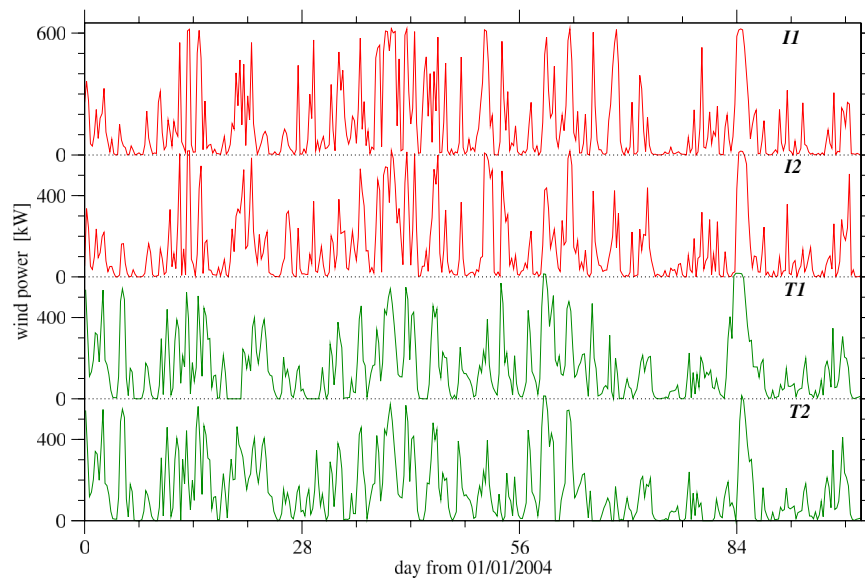


FIG. 8. Comparison of estimated electric output based on  $\alpha=1.529$  (see Fig. 5) and the power curve Eq. (3) from 6 h wind speed data for sites  $I1$  and  $I2$  (red) with direct measurements at the turbines  $T1$  and  $T2$  (green). Note that the latter two curves are 6 h averages of 10 min records.

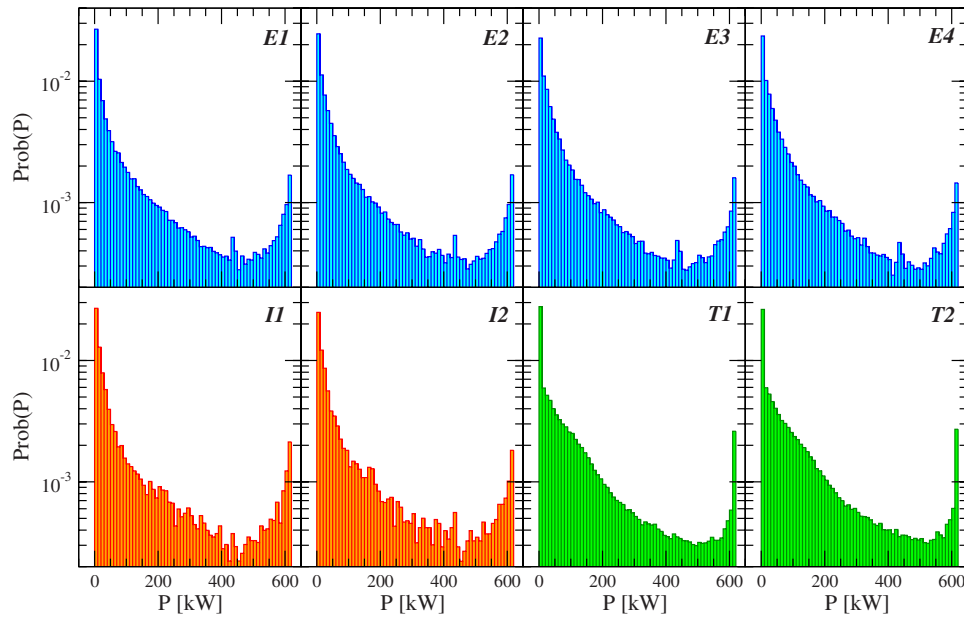


FIG. 9. Normalized histograms of electric power  $P$  for the time series  $E1, E2, \dots, T2$ . The last two (green) are based on direct measurements; the others are estimated by the power curve Eq. (3) from the rescaled surface wind speeds  $s' \rightarrow R_{T1} \times s$ , where the numerical value of  $R_{T1}$  is given in the second column of Table II. (The vertical scale is logarithmic.)

best result is provided by matching the long term average wind speed values  $\bar{s}$  listed in Table II, first column; numerical values of the appropriate multiplier  $R_{T1} = \bar{s}_{T1} / \bar{s}$  are given in the second column. Note that these factors impair the agreement for the wind speed histograms by giving too large frequencies to large values; however, this is fully indifferent from the point of view of power estimation because of the plateau regime (see Fig. 7).

Model and empirical output power histograms are shown in Fig. 9. The shape of the histograms is highly nontrivial; it is produced by the nonlinear transform of Eq. (3) from the empirical wind speed distributions in Fig. 4. It is no wonder that the best matching of turbine and reanalysis data is found for the closest site  $E1$ . Figure 10(a) illustrates the difference between the histograms of  $E1$  and  $T1$ ; the agreement is fairly good. The largest deviation is around very small but nonzero output power, where the frequency of appropriate wind speeds is over-represented in both ERA-40 and ERA-Interim data. The length of ERA-40 records permits to compute estimated annual ca-

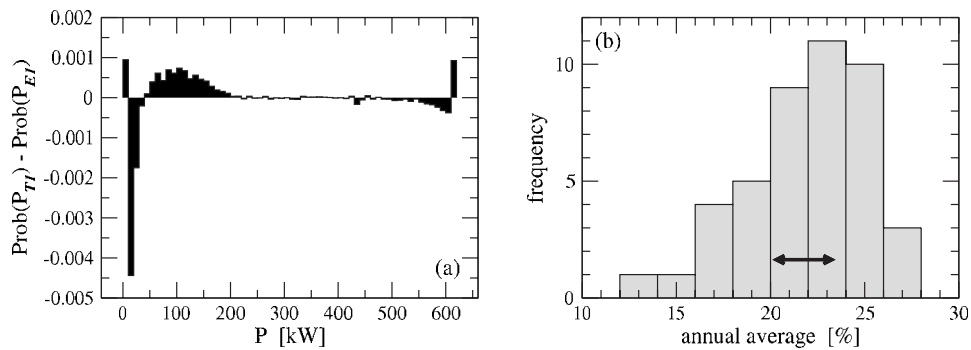


FIG. 10. (a) The difference between the histograms for sites  $T1$  and  $E1$  shown in Fig. 9. (b) Histogram of annual average output power estimated from the  $E1$  record by  $R_{T1} = 1.79$  and the power curve Eq. (3). The black arrow indicates the range of measured averages at  $T1$  and  $T2$ .

capacity factors for 43 whole years; the related histogram is shown in Fig. 10(b). The width of this histogram is surprisingly large; however, a comparison with reality would need much longer turbine records.

## VI. DISCUSSION

The goal of this work was to check the quality of ECMWF reanalysis wind fields near the ground from the point of view of wind energy estimates. Since reanalysis projects provide the longest available data sets of global spatial coverage, they might be extremely useful to evaluate large scale wind power potential. It is more common to use direct meteorological observations,<sup>2,4,11,37</sup> which are certainly more adequate considering local effects (wind microclimate); however, a remaining problem is the uneven spatial sampling.

Reanalysis procedures use smoothed orography, which is designed to avoid the Gibbs ripples due to spectral truncation;<sup>7</sup> thus the representation of surface irregularities with high spatial resolution is not possible. The resulting wind field is fairly coherent over large areas as demonstrated clearly in Sec. III. Comparisons with direct wind speed measurements at two turbines revealed that the dynamics is appropriately reproduced, apart from magnitudes. Note that this can be a consequence of the essentially flat surface configuration around the test site; much larger deviations between reanalysis and measured data are obtained over a complex terrain.<sup>10</sup>

A key point of wind power estimation from surface speed values is the approximation of speeds at hub heights. The scatter plot in Fig. 5(a) cannot disqualify the assumption of a linear relationship between 10 and 65 m data. The slope of the correlation line provides the simplest tool of speed estimates for the increased altitude. However, scaling with this factor results in an underestimated capacity profile, because shape anomalies of the wind speed histograms are amplified by the cubic section of the power curve Eq. (3). The best agreement for modeled and empirical histograms of output power is achieved when the long time average values of wind speed are matched; the corresponding multipliers are listed in Table II, second column. The apparent reason of this success is that such rescaling transforms the reanalysis histograms in a way that the best agreement is obtained for the modeled and measured wind speeds over the subplateau range of the power curve (0–13 m/s interval).

The mean wind profile, i.e., wind speed as a function of height averaged over a given period, is often described for engineering purposes by a power-law approximation,<sup>2,24,35,36</sup>

$$\frac{s(z_2)}{s(z_1)} = \left( \frac{z_2}{z_1} \right)^H, \quad (4)$$

where  $s(z_i)$  are the wind speeds at heights  $z_i$  and  $H$  is a characteristic exponent in the range 0.1–0.6. The matching factors used in this work (Table II, second column) are consistent with exponent values of 0.23–0.37. A widely known problem with this approach is that  $H$  varies with height, surface roughness, and stability.<sup>24,35,36</sup> A more realistic expression for the mean wind speed at height  $z$  is provided by the logarithmic wind profile with atmospheric stability correction.<sup>2,14,24</sup> Since stability considerations are beyond the scope of this work, we refer to the simplified logarithmic profile

$$\frac{s(z_2)}{s(z_1)} = \frac{\log(z_2/z_0)}{\log(z_1/z_0)}, \quad (5)$$

where  $z_0$  denotes a surface roughness length. The global average<sup>2</sup> is around  $\bar{z}_0 \approx 0.7$  m with a maximum of 3.5 m over complex terrains and with a minimum of a fraction of 1 mm over smooth orographies, such as sea surface. The factors in Table II correspond to roughness length values in the range of 0.3–1.6 m, which is also consistent with expectations.

An important consequence of the considerations above is that a uniform scaling factor cannot provide a satisfactory approximation of high altitude wind speeds for each location irrespective of the geographic conditions. It is very probable that the constant factor of 1.28 used by Kiss and Jánosi<sup>17</sup> seriously underestimates speed values over land, while it is too high for off-shore loca-

tions. The main problem is that changing wind speed probabilities in the range of most frequent moderate values (2–12 m/s) drastically affect an estimated capacity factor by cubic amplification, see Eq. (3) and Fig. 7. On the other hand, the present analysis confirms that the key parameter of wind power modeling is the long time average wind speed at potential hub heights, in agreement with Archer and Jacobson.<sup>2</sup>

Our main conclusion is that reanalysis wind data can provide reliable wind power estimates for extended geographic regions after proper parameter matching. We think that similar validation procedures for a couple of locations with various surface conditions would improve the utility of reanalysis records toward more accurate wind power estimates.

## ACKNOWLEDGMENTS

We thank the Hungarian Meteorological Service for the access to the ERA-40 data bank. This work was supported by the European Commission's DG RTD NEST Programme "Tackling Complexity in Science" (Contract No. 043363) and by the Hungarian Science Foundation (OTKA) under Grant No. NK72037.

- <sup>1</sup>J. Goldemberg, *Nature (London)* **456**, 26 (2008).
- <sup>2</sup>C. L. Archer and M. Z. Jacobson, *J. Geophys. Res.* **110**, D12110 (2005).
- <sup>3</sup>The world total primary energy consumption was  $\sim 15.5$  TW in 2005, according to the U.S. Energy Information Administration. <http://www.eia.doe.gov/>.
- <sup>4</sup>L. Landberg, L. Myllerup, O. Rathmann, E. L. Petersen, B. H. Jørgensen, J. Badger, and N. G. Mortensen, *Wind Energy* **6**, 261 (2003).
- <sup>5</sup>E. Kalnay, M. Kanamitsu, R. Kistler, W. Collins, D. Deaven, L. Gandin, M. Iredell, S. Saha, G. White, J. Woollen, Y. Zhu, M. Chelliah, W. Ebisuzaki, W. Higgins, J. Janowiak, K. C. Mo, C. Ropelewski, J. Wang, A. Leetmaa, R. Reynolds, R. Jenne, and D. Joseph, *Bull. Am. Meteorol. Soc.* **77**, 437 (1996).
- <sup>6</sup>M. Kanamitsu, W. Ebisuzaki, J. Woollen, S.-K. Yang, J. J. Hnilo, M. Fiorino, and G. L. Potter, *Bull. Am. Meteorol. Soc.* **83**, 1631 (2002).
- <sup>7</sup>S. M. Uppala, P. M. Kållberg, A. J. Simmons, U. Andrae, V. da Costa Bechtold, M. Fiorino, J. K. Gibson, J. Haseler, A. Hernandez, G. A. Kelly, X. Li, K. Onogi, S. Saarinen, N. Sokka, R. P. Allan, E. Andersson, K. Arpe, M. A. Balmaseda, A. C. M. Beljaars, L. van de Berg, J. Didlot, N. Bormann, S. Caires, F. Chevallier, A. Dethof, M. Dragosavac, M. Fisher, M. Fuentes, A. Hagemann, E. Holm, B. J. Hoskins, L. Isaksen, P. A. E. M. Janssen, R. Jenne, A. P. McNally, J.-F. Mahrouf, J.-J. Morcrette, N. A. Rayner, R. W. Saunders, P. Simon, A. Sterl, K. E. Trenberth, A. Untch, D. Vasiljevic, P. Viterbo, and J. Woollen, *Q. J. R. Meteorol. Soc.* **131**, 2961 (2005).
- <sup>8</sup>J. A. Francis, *Geophys. Res. Lett.* **29**, 1315 (2002).
- <sup>9</sup>B. N. Goswami and D. Sengupta, *J. Geophys. Res.* **108**, C3124 (2003).
- <sup>10</sup>M. Shrivani Kumar and V. K. Anandan, *Geophys. Res. Lett.* **36**, L01805 (2009).
- <sup>11</sup>C. L. Archer and M. Z. Jacobson, *J. Geophys. Res.* **108**, D4289 (2003).
- <sup>12</sup>S. M. Lazarus and J. Bewley, *J. Geophys. Res.* **110**, D07102 (2005).
- <sup>13</sup>S. Emeis and M. Türk, *Wind Energy: Proceedings of the Euromech Colloquium* (Springer-Verlag, Berlin, 2007), p. 61.
- <sup>14</sup>A. Dhanju, P. Whitaker, and W. Kempton, *Renewable Energy* **33**, 55 (2008).
- <sup>15</sup>H.-T. Mengelkamp, *Theor. Appl. Climatol.* **63**, 129 (1999).
- <sup>16</sup>S. C. Pryor, J. T. Schoof, and R. J. Barthelmie, *J. Geophys. Res.* **110**, D19109 (2005).
- <sup>17</sup>P. Kiss and I. M. Jánosi, *Nonlinear Processes Geophys.* **15**, 803 (2008).
- <sup>18</sup>P. Kiss and I. M. Jánosi, *Energy Convers. Manage.* **49**, 2142 (2008).
- <sup>19</sup><http://www.ecmwf.int/research/era/do/get/era-interim>.
- <sup>20</sup>T. Liszka, *Int. J. Numer. Methods Eng.* **20**, 1599 (1984).
- <sup>21</sup>A. Dadpay, E. S. Soofi, and R. Soyer, *J. Econometr.* **138**, 568 (2007).
- <sup>22</sup>K. Conradson and L. B. Nielsen, *J. Appl. Meteorol.* **23**, 1173 (1984).
- <sup>23</sup>B. Dodson, *The Weibull Analysis Handbook*, 2nd ed. (ASQ Quality, Milwaukee, 2006).
- <sup>24</sup>E. L. Petersen, N. G. Mortensen, L. Landberg, J. Højstrup, and H. P. Frank, *Wind Energy* **1**, 2 (1998).
- <sup>25</sup>S. E. Gryning, H. Jørgensen, S. Larsen, and E. Batchvarova, *J. Phys.: Conf. Ser.* **75**, 012066 (2007).
- <sup>26</sup>*Observed Global Climate*, edited by M. Hantel (Springer-Verlag, Berlin, 2005).
- <sup>27</sup>S. C. Pryor and R. J. Barthelmie, *Wind Energy* **4**, 173 (2001).
- <sup>28</sup>A. R. Henderson, C. Morgan, B. Smith, H. C. Srensen, R. J. Barthelmie, and B. Boesmans, *Wind Energy* **6**, 35 (2003).
- <sup>29</sup>R. Barthelmie, O. F. Hansen, K. Enevoldsen, J. Højstrup, S. Frandsen, S. Pryor, S. Larsen, M. Motta, and P. Sanderhoff, *J. Sol. Energy Eng.* **127**, 170 (2005).
- <sup>30</sup>K. Tar, L. Makra, S. Horváth, and A. Kircsi, *Theor. Appl. Climatol.* **69**, 69 (2001).
- <sup>31</sup>J. Bartholy, K. Radics, and F. Bohoczky, *Renewable Sustainable Energy Rev.* **7**, 175 (2003).
- <sup>32</sup>L. Varga, Z. Korényi, and T. Hirsch, *WSEAS Trans. Power Syst.* **1**, 1243 (2006).
- <sup>33</sup>T. Weidinger, A. Kiss, A. Z. Gyöngyösi, K. Krassován, and B. Papp, *Wind Energy: Proceedings of the Euromech Colloquium* (Springer-Verlag, Berlin, 2007), p. 167.
- <sup>34</sup>K. Radics and J. Bartholy, *Renewable Sustainable Energy Rev.* **12**, 874 (2008).
- <sup>35</sup>T. Burton, D. Sharpe, N. Jenkins, and E. Bossanyi, *Wind Energy Handbook* (Wiley, Chichester, 2001).
- <sup>36</sup>E. Hau, *Wind Turbines. Fundamentals, Technologies, Application, Economics*, 2nd ed. (Springer-Verlag, Berlin, 2006).
- <sup>37</sup>G. Giebel, *Wind Energy* **10**, 69 (2007).